Electronic Supplementary Material (ESI) for Journal of Materials Chemistry A.

Electronic Supplementary Materials

Fe_2P/reduced graphene oxide/Fe_2P sandwich-structured nanowall arrays: a high-performance non-noble-metal electrocatalyst for hydrogen evolution

Meijun Liu[a], Liming Yang[a,c], Tian Liu[a], Yanhong Tang[b,*], Shenglian Luo[a,c], Chengbin Liu[a,*], Yunxiong Zeng[a]

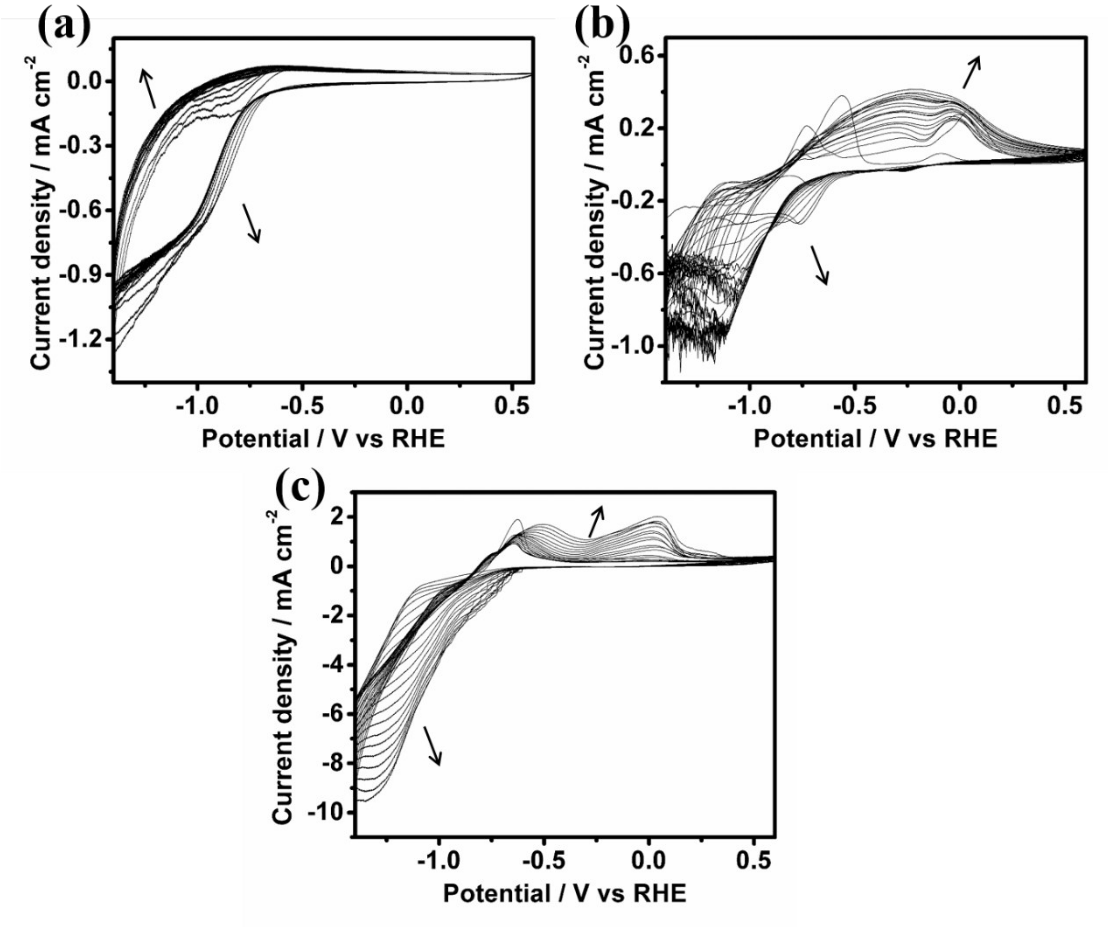

Fig. S1 CV curves for electrolyzing (a) colloidal solution of GO, (b) the Fe precursor composed of $FeSO_4$ and $Na_2S_2O_3$, and (c) GO/Fe precursor colloidal solution on Ti plates performed in the potential range between −1.4 and 0.6 V *versus* SCE for 20 cycles. The arrows point to the increase of the peak current densities, meaning the deposition of the conductive materials.

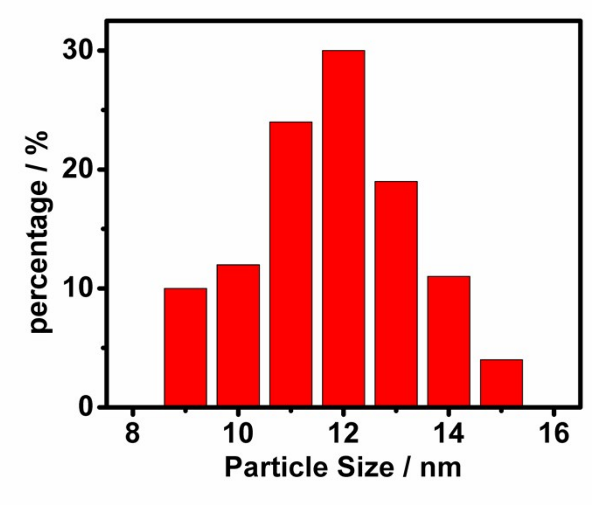

Fig. S2 Histogram of statistical analysis of Fe_2P particle size (based on 100 randomly picked particles).

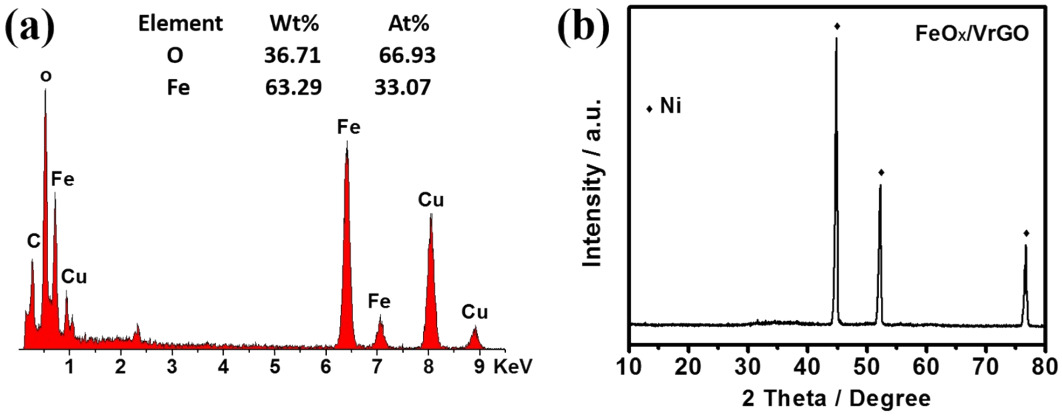

Fig. S3 (a) EDX and (b) XRD pattern of FeO_x@rGO.

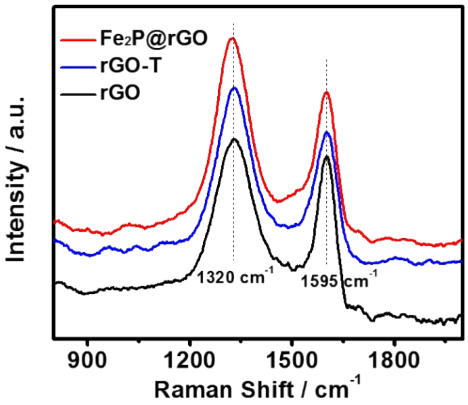

Fig. S4 Raman spectrum of Fe_2P@rGO, rGO-T and rGO. The D and G bands are indicative of the graphene moiety.

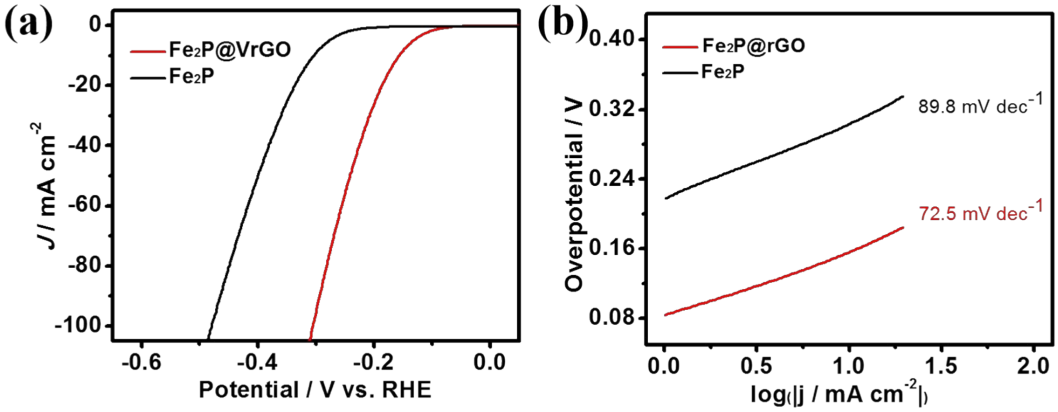

Fig. S5 (a) Polarization curves and (b) corresponding Tafel plots for the different materials in N_2-saturated 1.0 M NaOH solution at a scan rate of 2 mV s^{-1};

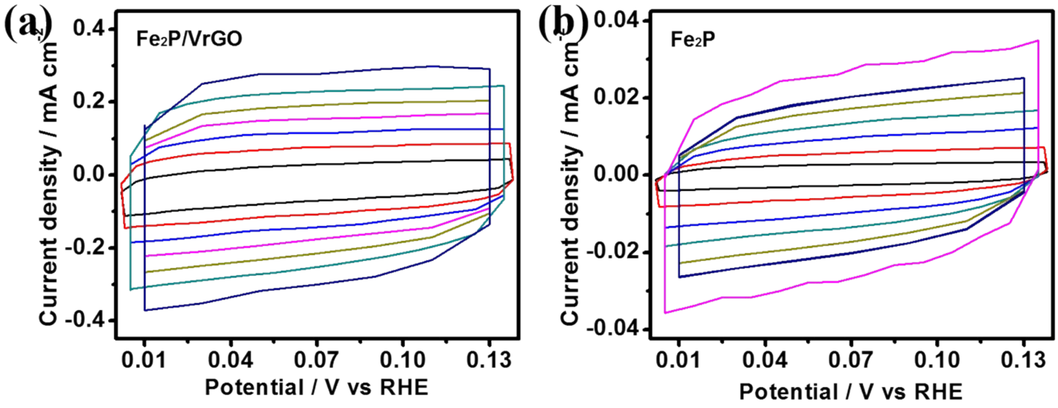

Fig. S6 Cyclic voltammetry curves of (a) Fe_2P@rGO,and (b) Fe_2P in the range of 0-0.14 V vs. RHE. The scan rate is 40, 80, 120, 160, 200, 240, and 300 mV $s^{-1}$for the curves from inside to outside.

As shown in Fig. S7, R_s represents the ohmic resistance arising from the electrolyte and all contacts. The time constant R1-CPE may relate to the interfacial resistance resulting from the electron transport between the cataysis and the Ti plate, the higher CPE can further indicate the specific surface area of Fe_2P@rGO (Table S1). Q and R_{ct} are assigned as the double-layer capacitance and charge-transfer resistance at the interface between the cataysis and the electrolyte, which generally represents the electrochemical activity of the electrode.

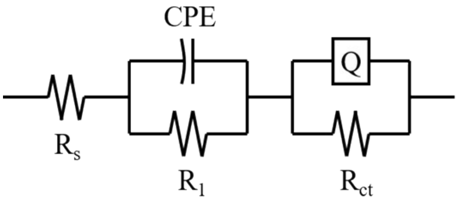

Fig. S7 Equivalent circuit used for fitting the Nyquist plots in Figure 4d.

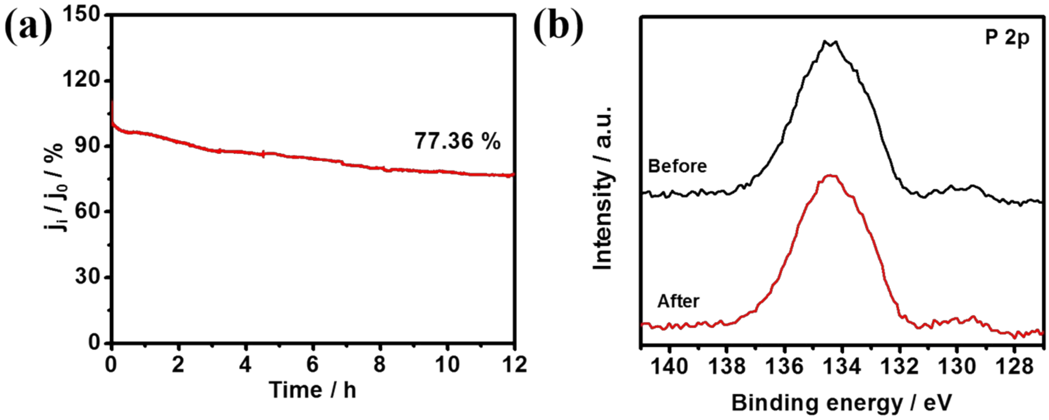

Fig. S8 (a) Current-time curve of Fe_2P@rGO in 0.5 M H_2SO_4 solution at an overpotential of 300 mV for 12 h (b) XPS spectra of P 2p before and after 5000 cycles test.

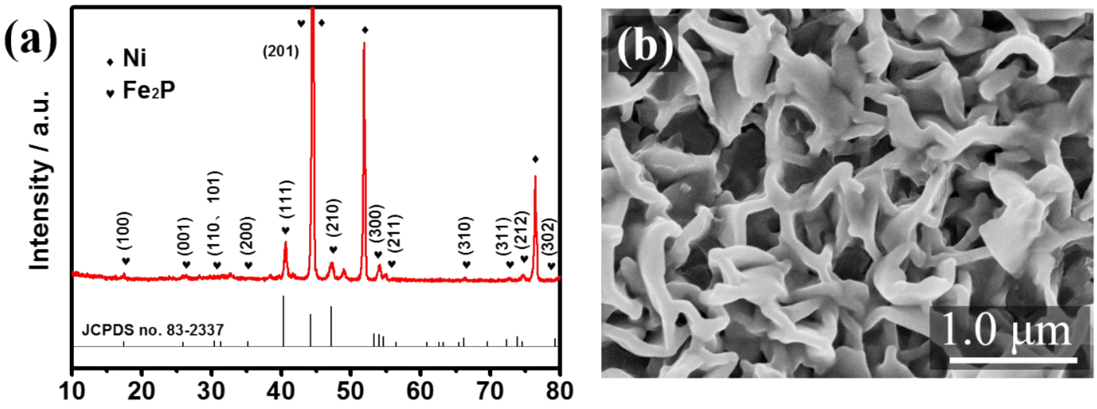

Fig. S9 (a) SEM images and (b) XRD pattern of Fe$_2$P@rGO after 5000 cycles test.

Calculation of active sites

The number of active sites are calculated from the cyclic voltammograms without faradic current in **Figure S5** at the rate of 200 mV s^{-1} by integrating the current over the whole potential. Later, the absolute components of the voltammetric charges (cathodic and anodic) reported during one single blank measurement were added. Assuming a one electron redox process, this absolute charge was divided by two. The value was then divided by the Faraday constant to get the number of active sites of the film. The total number of active sites for each catalyst can be calculated from cyclic voltammetry by integrating the current over the whole potential.

The number of active sites = Area under the curve / 2F

The calculated number of active sites for the electrode materials are,

$$n\,(Fe_2P@rGO) = 1.0 \times 10^{-3} mol\ g^{-1}$$

$$n\,(Fe_2P) = 8.0 \times 10^{-5} mol\ g^{-1}$$

Determination of the turnover frequency (TOF)

When the number of active sites is known, the turnover frequencies (in s^{-1}) were calculated with the following equation:

$$TOF = \frac{j\ 1}{Fn2}$$

j: Current (in A) during the linear sweep measurement at $\eta = 200$ mV.

F: Faraday constant (in C/mol).

n: Number of active sites (in mol) calculated as the method above.

The factor ½ arrives by taking into account that two electrons are required to form one hydrogen molecule from two protons.

$$TOF(Fe_2P@rGO) = \frac{100.80\,mA\,cm^{-2} \qquad 1}{96485.34\,C\,mol^{-1}\,1.0 \times 10^{-3}\,mol\,g^{-1}\,0.47\,mg\,cm^{-2}2}$$

$$TOF(Fe_2P) = \frac{2.44\,mA\,cm^{-2} \qquad 1}{96485.34\,C\,mol^{-1}8.0 \times 10^{-5}\,mol\,g^{-1}\,0.47\,mg\,cm^{-2}2}$$

Table S1. Electrochemical impedance parameters obtained by fitting the Nyquist plots to the equivalent circuit model (Figure S6).

Catalyst	R_s (Ω)	C_1 (mF cm^{-2})	R_1 (Ω)	Q		R_{ct} (Ω)
				$Y_1(\Omega^{-1}s^n)$	n	
Fe_2P@rGO	19.67	0.163	286.8	7.403×10^{-5}	0.8864	248.4
Fe_2P	28.18	0.072	330.0	16.9×10^{-5}	0.8891	4563

Table S2. Comparison of HER activity of some transition metal phosphides.

Catalyst	Current density (mA·cm^{-2})	Potential (mV)	Tafel slope (mV·dec^{-1})	Reference
Fe_2P@rGO	10	101	55.2	This work
	20	122		
Fe-	10	104	58	1
CoP/CNTs	10	165	68	2
$Co_{1.6}Ni_{0.4}P$/CNT	20	118.8	68.2	3
Ni-Co-P-300	10	150	60.6	4
Ni_2P/CNT	10	124	41	5
Ni_5P_4 solid NPs	10	118	42	6
Ni_2P/NRGO	10	102	59	7
Ni_2P/CNSs-20	10	107	49	8
Ni_2P	20	130	46	9

1 Y. Pan, Y. Liu, Y. Lin and C. Liu, *ACS Appl. Mater. Interfaces*, 2016, **8**, 13890-13901.

2 Y. Zheng, Y. Jiao, M. Jaroniec and S. Z. Qiao, *Angew. Chem. Int. Ed.*, 2015, **54**, 52-65.

3 Y. Pan, Y. Chen, Y. Lin, P. Cui, K. Sun, Y. Liu and C. Liu, *J. Mater. Chem. A*, 2016, **4**, 14675-14686.

4 Y. Feng, X. Y. Yu and U. Paik, *Chem. Commun.*, 2016, **52**, 1633-1636.

5 Y. Pan, W. Hu, D. Liu, Y. Liu and C. Liu, *J. Mater. Chem. A*, 2015, **3**, 13087-13094.

6 Y. Pan, Y. Liu, J. Zhao, K. Yang, J. Liang, D. Liu, W. Hu, D. Liu, Y. Liu and C. Liu, *J. Mater. Chem. A*, 2015, **3**, 1656-1665.

7 Y. Pan, Y. Liu and C. Liu, *J. Power Sources*, 2015, **297**, 45-52.

8 Y. Pan, N. Yang, Y. Chen, Y. Lin, Y. Li, Y. Liu and C. Liu, *J. Power Sources*, 2015, **285**,169-177.

9 F. C. Juan, G. R. Carlos, W. R. Christopher, S. L. Nathan and E. S. Raymond, *Chem. Mater.*, 2016, **28**, 6017-6044.